

# Assessment of Terrestrial Radioactivity Distribution in Olkaria Geothermal Field, Kenya

Solomon Namaswa\*<sup>1</sup>, Nicholas Mariita<sup>1</sup>, Douglas Onyancha<sup>2</sup> and Judith Kananu<sup>3</sup>

<sup>1</sup>Geothermal Training and Research Institute, Dedan Kimathi University of Technology, Nyeri, Kenya

<sup>2</sup>Department of Chemistry, Dedan Kimathi University of Technology, Nyeri, Kenya

<sup>3</sup>Department of Chemistry, University of Nairobi, Kenya, Nyeri, Kenya

## ABSTRACT

Geothermal energy has played a major role in energy supply in Kenya and even overtaking other forces of energy. However, utilization of subsurface fluids need comprehensive examination and the results communicated to the general public. This is because natural radiation is considered critical during earth processes since the gradual disintegration of naturally occurring radioactive elements account for almost half of the energy that brings about volcanology processes. This therefore implies that the slow decay of radioactive elements aids in generation of temperature gradient beneath the earth surface. In this survey, NaI(Tl) gamma-ray spectrometer was employed in determination of the NORMs levels within the Olkaria geothermal field and estimated the hazards indices that arise from the decay of these products in relation to other physico-chemical parameters such as temperature, TOC, pH and specific gravity. The study revealed that <sup>238</sup>U, <sup>232</sup>Th and <sup>40</sup>K had average levels at  $66.42 \pm 16.02 \text{ Bqkg}^{-1}$ ,  $46.92 \pm 9.52 \text{ Bqkg}^{-1}$  and  $512.84 \pm 226.49 \text{ Bqkg}^{-1}$  respectively while  $80.56 \pm 17.77 \text{ nGyh}^{-1}$ ,  $0.1 \text{ mSvy}^{-1}$ ,  $0.47$  and  $172.79 \pm 30.37 \text{ Bq/Kg}$  were the mean values for absorbed dose rates, annual effective dose rate, hazard index and radium equivalent respectively. Also a weak positive correlation between pH, TOC and s.g and the concentration of the three radioactive elements was observed. From the obtained results, the studied hazard indices were below the world acceptable safety limits and therefore human exposure to radiation is within safety levels. Also change in physicochemical parameters does not affect the radionuclide concentrations. This shows that the exploitation of geothermal energy in Olkaria has not affected the activity concentration level of <sup>238</sup>U, <sup>232</sup>Th and <sup>40</sup>K and the hazard indices.

**Keywords:** Annual Effective Dose, Internal Hazard Index, Radium Equivalent, Kenya.

## I. INTRODUCTION

The two main causes of high temperature in the earth subsurface are heat that was generated during the creation of the planet when heavenly bodies pumped into each other and the liquefied sphere split into dense inner layers and less dense outer layers [1]. Due to low heat loss from the earth, the temperature has been kept high in the core and mantle for more than the 4.6 billion years the earth has been in existence [1]. Also, high temperature beneath the subsurface generated from the radioactive decay of natural

radioactive elements such as <sup>238</sup>U, <sup>40</sup>K and <sup>232</sup>Th according to [2]. This process of decay is crucial for earth systems since the slow decay of radioactive elements is estimated to produce approximately half of the heat that drives major earth processes such as continental drift, ocean spreading and plate tectonics [3].

Therefore, in Earth's continental crust, the radioactive decay of natural radioactive elements has had an involvement in the origin of geothermal heat [2] with major heat-producing isotopes being <sup>238</sup>U,

$^{235}\text{U}$ ,  $^{40}\text{K}$ , and  $^{232}\text{Th}$  [4] and [5] as shown in figure 1 below.

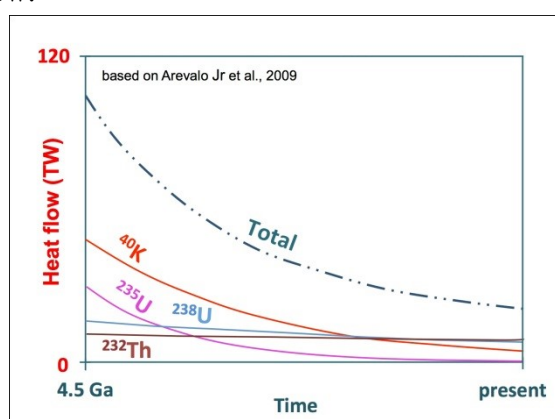


**Figure 1.** The radiogenic heat from the decay of  $^{238}\text{U}$ ,  $^{40}\text{K}$ ,  $^{235}\text{U}$  and  $^{232}\text{Th}$  as major contributors to the earth's internal heat budget [5]

Olkaria geothermal field in the Kenyan East African Rift being the most productive geothermal field according to [6] was hence studied for the purposes of assessment of natural radiation systematics. Because of the rock interactions with the beneath intrusions of magma that heats them, surface rocks may have higher levels of the naturally occurring radioactive materials that could impact this region.

## II. METHODS AND MATERIAL

### 2.1 The Area of Study

The Greater Olkaria geothermal area is situated on the foot of the Kenya rift in the southern part nearly 95Km from Nairobi (figure 2) and is part of the structure of the East African rift which extends from Afar triple junction in the northern part of Ethiopia to Mozambique region in the south [7]. It forms a section of the eastern arm of the rift that extends from Lake Turkana to Lake Natron, [8].

The Greater Olkaria volcanic complex is distinguished by various volcanologies of Pleistocene and the Holocene ages [9]. Other Pleistocene and the Holocene volcanic centres adjacent to Olkaria as shown in figure 2 are among Longonot volcano to the southeast, Suswa caldera to the south, and the Eburru volcanic complex to the north.

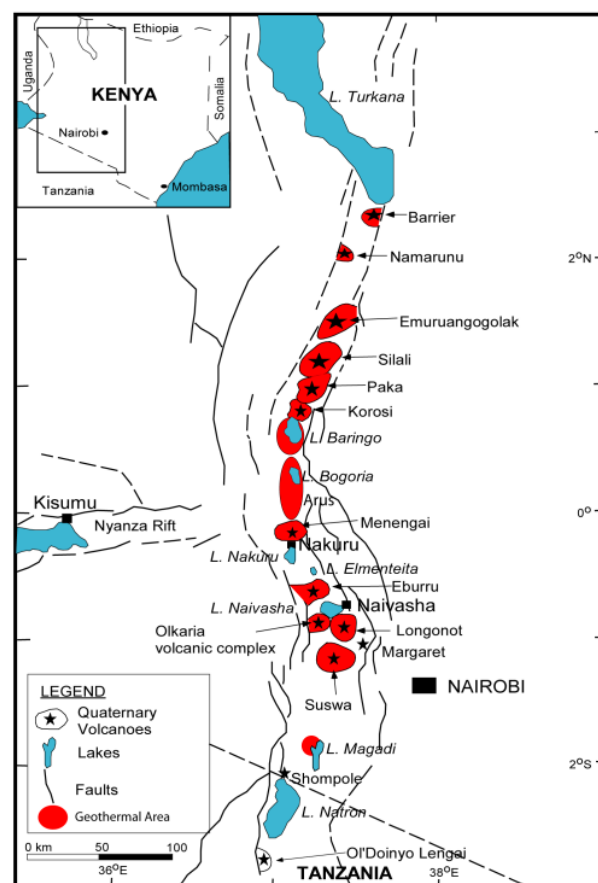


**Figure 2.** Map of the Kenya rift displaying location of Olkaria and other volcanoes [18].

### 2.2 Data collection and preparation

Rock samples near the fumaroles sites along Ololbutot fault within the greater Olkaria geothermal field were collected.

The rock and sediment samples were opened and air dried for a one week period before being crunched and mashed into finer powder to ensure homogeneity in the samples. The samples were then transferred into numbered plastic containers, measured and closed to prevent gaseous  $^{220}\text{Rn}$  and  $^{222}\text{Rn}$  from escape. For every site, two sets of jars were set up for each of the rock and sediment samples. The samples' weights were then recorded and stored for two weeks to allow for secular equilibrium achievement between  $^{226}\text{Ra}$  and the decay products of  $^{222}\text{Rn}$  ( $^{214}\text{Bi}$  and  $^{214}\text{Pb}$ ) and the in-growth of gaseous  $^{222}\text{Rn}$  before analysis using gamma-ray was done [10]. A background sample was also prepared by sealing distilled water in a similar jar. Distilled water was chosen because it is

considered a blank reference standard hence appropriate for background correction.

### 2.3 Activity Concentration

The specific activity of a nuclide was measured using the given equation

$$C_n = N_n(\gamma_d \times \eta_E \times T \times m) \quad (1)$$

where  $C_n$  is the activity concentration (in Bq/kg) of the radionuclide  $n$  for a peak at energy  $E$ ,  $N_n$  is the net counts of a nuclide  $n$  in a peak at energy  $E$ ,  $T$  is the counting time for a sample,  $\gamma_d$  is the gamma ray abundance per disintegration of the specific nuclide at energy  $E$ ,  $m$  is the mass (in kg) of sample and  $\eta_E$  is the detection efficiency of crystal at energy  $E$ .

### 2.3 Determination of radium equivalent activity

Radium equivalent activity gives a single index, which express the gamma yield from various mixture of  $^{226}\text{Ra}$ ,  $^{232}\text{Th}$  and  $^{40}\text{K}$  in the sample. The radium equivalent activity index was given as:

$$Ra_{eq}(\text{Bq/kg}) = C_U(\text{Bq/kg}) + 1.43C_{Th}(\text{Bq/kg}) + 0.077C_K(\text{Bq/kg}) \quad (2)$$

where  $C_U$ ,  $C_{Th}$  and  $C_K$  were the radioactivity concentration in  $\text{Bqkg}^{-1}$  of  $^{238}\text{U}$ ,  $^{232}\text{Th}$ , and  $^{40}\text{K}$ . It may be noted the decay product of  $^{226}\text{Ra}$  replaced that  $^{238}\text{U}$ , although there may be disequilibrium between  $^{238}\text{U}$  and  $^{226}\text{Ra}$  [11]. It is accepted that 370  $\text{Bqkg}^{-1}$  of  $^{238}\text{U}$  or 259  $\text{Bqkg}^{-1}$  of  $^{232}\text{Th}$  or 4810  $\text{Bqkg}^{-1}$  of  $^{40}\text{K}$  produces the same gamma dose rate [12]. The maximum value of  $Ra_{eq}$  must be less than 370  $\text{Bqkg}^{-1}$ .

### 2.4 External hazard index

The external exposure is caused by direct gamma radiation whereas internal exposure is caused by the inhalation of radon ( $^{222}\text{Rn}$ ), thoron ( $^{220}\text{Rn}$ ) and their short-lived decay products [13]. For the estimation of gamma radiation dose measurement anticipated that is conveyed externally from building materials, the external hazard index ( $H_{ex}$ ) is measured by equation [14]:

$$H_{ex} = \frac{C_U}{370} + \frac{C_{Th}}{259} + \frac{C_K}{4810} \quad (3)$$

The external hazard index should be less than unity to stay the radiation risk to be minimum, which is equivalent to a maximum value of Radium equivalent 370 Bq/kg.

### 2.5. Annual effective dose

The expected annual effective dose received by the population attributable to radioactivity in soil is estimated employing a conversion factor of 0.7 Sv/Gy. The adults spend about 80% of their time indoors, while the remaining 20% time is spent outdoors. Therefore, the outdoor occupancy factors were given as 0.2, hence the outdoor annual effective dose rate was calculated by equation 4 [15].

$$D_{out}(\text{mSvY}^{-1}) = D(\text{nGyY}^{-1}) \times 8670\text{h} \times 0.2 \times 0.7(\text{SvGy}^{-1}) \times 10^{-6} \quad (4)$$

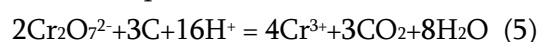
### 2.6 Determination of Sample pH

The weight of the samples were taken and the samples mixed with distilled water in the water to soil ratio of 1:1 of their weight in the laboratory according to [16]. and the mixture was stirred until a slurry was obtained and then covered with watch glass. In order to let the samples pH to remain the same, the samples stood for at least one hour, stirring after every 12 minutes while taking the Soil pH using pH meter and the average values of pH calculated.

### 2.7 Determination of Total Organic Carbon by Wet Chemistry Technique

According to [16], concentrated sulphuric acid and Potassium dichromate were added to 0.5 g of samples and the solution was gently heated at about 150°C for approximately 30 minutes. Then the mixture was swirled and allowed to cool due to the exothermic reaction process when the potassium dichromate and sulphuric acids were mixed before addition of water to stop the process. Gentle boiling at a controlled temperature allowed complete oxidation of organic Carbon. After the solution had cooled,  $\text{H}_3\text{PO}_4$  was added to the mixture so as to aid in elimination of interferences from the ferric ( $\text{Fe}^{3+}$ ) iron which were

present in the sample [17]. The chemistry behind this extraction procedure is as follows:



Manual titration was performed to determine the quantity of organic carbon present in the soil where Ortho-phenanthroline ferrous complex (commercially available as "Feroin") indicator solution was added to the digest [25]. Then the excess  $\text{Cr}_2\text{O}_7^{2-}$  was titrated with ferrous ammonium sulphate [ $\text{Fe}(\text{NH}_4)_2(\text{SO}_4)_2 \cdot 6\text{H}_2\text{O}$ ] until colour in the sample changed from green to reddish brown.

### III. RESULTS AND DISCUSSION

#### 3.1 Activity Concentrations

The activity concentrations of the three radionuclides K40, U238 and Th232 from every sampling site were calculated (table 1) in which the average for K40,

U238 and Th232 are  $512.84 \pm 226.49 \text{Bqkg}^{-1}$ ,  $66.42 \pm 16.02 \text{Bqkg}^{-1}$  and  $46.92 \pm 9.52 \text{Bqkg}^{-1}$  respectively.

From the results, disparities in the levels of the radionuclides from one sampling point to the other was noticed. This was attributed to the different rock formations in the region that could have resulted into different concentrations of the measured radionuclides according to [18].

The mean activities of  $^{40}\text{K}$ ,  $^{238}\text{U}$  and  $^{232}\text{Th}$  in rock samples from the field of study were marginally above the world recommended safety values of  $400 \text{BqKg}^{-1}$ ,  $35 \text{Bq Kg}^{-1}$  and  $30 \text{BqKg}^{-1}$  respectively [15]. This could be linked with mylonitized granite gneiss, augen, garnetiferous mica schist and micaceous weathered quartzite, and tectonically emplaced magmatic bodies [19].

**Table 1.** Activity concentrations of the natural radionuclides in samples

site	$^{40}\text{K}$	$^{238}\text{U}$	$^{232}\text{Th}$
S1	630.86±4.60	61.33±2.91	41.86±2.02
S2	757.27±2.92	76.67±0.33	36.535±3.77
S3	632.69±29.66	43.41±4.16	38.79±0.23
S4	620.21±2.85	84.56±4.6	57.66±0.35
S5	848.77±4.99	82.585±2.86	66.93±1.8
S6	236.13±17.64	53.83±3.36	56.25±5.39
S7	167.455±8.68	44.57±0.76	43.55±0.78
S8	473.17±11.02	53.66±4.32	38.665±1.46
S9	196.085±8.01	77.095±0.71	47.09±1.99
S10	565.75±11.67	86.49±4.23	41.92±1.99
<b>Mean</b>	<b>512.84±226.49</b>	<b>66.42±16.02</b>	<b>46.92±9.52</b>

#### 3.2 Hazard Indices

The AEDR, Hex, Raeq and absorbed dose rate (D) values were all calculated for all the sampling sites (table 2) in which mean of  $0.10 \pm 0.02 \text{mSvy}^{-1}$  for

AEDR was obtained. Hazard index (Hex) of  $0.47 \pm 0.08$ , radium equivalent value of  $172.79 \pm 30.37 \text{Bqkg}^{-1}$  and absorbed dose rate value of  $81.35 \pm 14.61 \text{nGy/h}$  averages was found.

**Table 2.** Average for radiological parameters of the natural radionuclides in rock samples

site	D(nGy/h)	Hex	AEDR	Raeq
S1	81.79	0.47	0.10	172.98
S2	88.77	0.51	0.12	187.07
S3	71.69	0.41	0.09	150.51
S4	92.68	0.54	0.11	198.74
S5	117.30	0.68	0.14	250.20
S6	70.68	0.42	0.09	155.38
S7	60.62	0.36	0.07	133.87
S8	62.27	0.36	0.08	133.48
S9	77.72	0.46	0.10	171.03
S10	90.00	0.52	0.11	174.64
<b>Mean</b>	<b>81.35±14.61</b>	<b>0.47±0.08</b>	<b>0.10±0.02</b>	<b>172.79±30.37</b>

The values obtained fall below the limits of these indices in this study, which is of inconsequential radiation risk to the community within the area, and perilous effect of carcinogenic radon and its short-lived progeny is irrelevant to the human population [15].

### 3.3 Physico-chemical properties

Total organic carbon was analyzed field ranged from 8.4% to 12.88% (Table 3). A weak negative correlation between  $^{238}\text{U}/\text{TOC}$  and  $^{40}\text{K}/\text{TOC}$  and a weak positive correlation between  $^{232}\text{Th}/\text{TOC}$  was observed as shown in Table 4. This implies that the change in rocks TOC does not affect the

concentrations of the naturally occurring radioactive elements.

Specific gravity in the samples from Olkaria field at different sampling points was determined as shown in Table 3. Olkaria field recorded a Specific gravity that ranged from 1.023 to 1.029. A weak positive correlation between Specific gravity and the concentration of the three radioactive elements was observed as shown in Table 4. This implies that the change in rocks TOC does not affect the concentrations of the naturally occurring radioactive elements.

**Table 3.** Physico-chemical properties

site	pH	TOC (%)	s.g	T°C
S1	9.8±0.66	11.32	1.023	73.4
S2	9.6±0.14	11.81	1.024	66.8
S3	10.5±0.57	10.5	1.025	79.6
S4	9.7±0.50	11.69	1.029	84.7
S5	9.8±0.42	8.4	1.025	46.2
S6	9.6±0.29	12.88	1.025	53.1
S7	9.6±0.37	11.73	1.023	83.7
S8	10.3±0.33	11.51	1.025	84.5
S9	9.6±0.37	10.93	1.025	61.8
S10	9.9±0.62	9.67	1.024	75.2

Temperature measurements in samples from Olkaria field at different sampling points were determined as shown in Table 3. Olkaria field sediments recorded temperature that ranged from 84.7°C to 46.2° C. A weak positive correlation between temperature and

the concentration of the three radioactive elements was observed as shown in Table 4.10. The weak correlation shows that the change in temperature does not affect the radionuclide concentrations.

**Table 4.** correlation of radionuclide concentrations and physicochemical properties

Correlated Radionuclides	Correlation Coefficient( R)
U-238/pH	0.37
U-238/s.g	0.39
U-238/TOC	-0.16
U238/T	0.18
Th-232/pH	0.12
Th-232/s.g	0.23
Th-232/TOC	0.07
Th 232/T	0.27
K-40/pH	0.28
K-40/s.g	0.14
K-40/TOC	-0.28
K40/T	0.19

#### IV. CONCLUSION

Average activity concentration of the measured radionuclides falls within the world safety values. A large variation of activity concentrations observed at different locations of study area was attributed to differences in mineralogical content present in rocks as a result of regional geology of study area.

The total annual effective dose is below the average level of 1mSv/y as recommended by [15 and 24]. External hazard index and internal hazard index for all samples investigated are within recommended safety limits and hence do not pose any radiation hazards to the inhabitants.

#### V. REFERENCES

- [1]. Alfe, D., Gillan, M. J., Vocadlo, L., Brodholt, J. and Price, G. D. (2002). The Ab Initio Simulation of the Earth's. *Phil, Trans. R. Soc. Lond.* 360, 1227-1244
- [2]. Kelley, S. (2010). *Geothermal Energy*, *Lite Geology*. New Mexico Bureau of Geology & Mineral Resources, a Division of New Mexico Tech
- [3]. Fowler, C.M.R. (1990). *The Solid Earth: An Introduction to Global Geophysics*. Cambridge University Press.
- [4]. Turcotte, D. L. and Schubert, G. (2002). *Geodynamics (2nd Ed.)*. Cambridge, England, UK: Cambridge University Press. p. 137.
- [5]. Arevalo, R. D., W. F. McDonough, and M. Luong. (2009). The K/U ratio of the silicate Earth: Insights into mantle composition, structure and thermal evolution. *Earth and Planetary Science Letters*, 278: 361-369
- [6]. Ouma, P.A. (2009). *Geothermal Exploration and Development of the Olkaria Geothermal Field*. Presented at Short Course IV on Exploration for Geothermal Resources, organized by UNU-GTP, KenGen and GDC, at Lake Naivasha, Kenya.
- [7]. Kandie, R.J. (2014). *Eastern Rift Structural Geology-Tectonics, Volcanology and Geothermal* Presented at Short Course IX on Exploration for Geothermal Resources, organized by UNU-GTP,

- GDC and KenGen, at Lake Bogoria and Lake Naivasha, Kenya.
- [8]. Omenda, P.A. (2008). Status of Geothermal Exploration in Kenya and Future Plans for Its Development. Presented at Short Course III on Exploration for Geothermal Resources, organized by UNU GTP and KenGen, at Lake Naivasha, Kenya.
- [9]. Lagat, J.K. (2004). Geology, Hydrothermal Alteration And Fluid Inclusion Studies Of Olkaria Domes Geothermal Field, Kenya. Msc. Thesis, University of Iceland
- [10]. Ramasamy V, Senthil S., Meenakshisundaram V. and Gajendran V. (2009). Measurement of Natural Radioactivity in Beach Sediments from North East Coast of Tamilnadu, India, *Resource Journal on Appropriate Technology and Scientific Engineering*, 1 (2): 54-58.
- [11]. Iqbal, M., Tufail, M., & Mirza, S. M. (2000). Measurement of natural radioactivity in marble found in Pakistan using NaI(Tl) gamma-ray spectrometer. *Journal of Environmental Radioactivity*, 51, 255-265.
- [12]. Yu, K. N., Guan, Z. J., Stoks, M. J., & Young, E. C. (1992). The assessment of natural radiation dose committed to the Hong Kong People. *Journal of Environmental Radioactivity*.
- [13]. Turhan, S., & Varinlioglu, A. (2012). Radioactivity measurement of primordial radionuclides in and dose evaluation from marble and glazed tiles used as covering building materials in Turkey. *Radiation Protection Dosimetry* 546-555.
- [14]. Beretka, J., & Mathew, P. J. (1985). Natural radioactivity of Australian building materials, waste and by-products. *Health Physics*, 48, 87-95.
- [15]. UNSCEAR, (2000). Sources and Effects of Ionizing Radiation; United Nation Scientific Committee on the Effects of Atomic Radiation Annex A.B. New York.
- [16]. Kananu, J., Madadi, V.O. and Kamau, G.N. (2014). Impact of Long Term Inorganic Fertilization with Emphasis on Heavy Metals, Soil pH and Total Organic Carbon on Maize Farm Soils in Trans Nzoia, Kenya. *The International Journal of Science & Technology*, 2(11), 183-188
- [17]. Tiessen H. and J.O. Moir. 1993. Total and Organic Carbon. In: *Soil Sampling and Methods of Analysis*. M.E. Carter, Ed. Lewis Publishers, Ann Arbor, MI. p. 187-211.
- [18]. Namaswa, S.W., Okoth, C.O. and Makori, B. (2017). Analysis of Natural Radioactivity and Radiation Exposure Levels in Eburru Geothermal Field, Kenya. *IJSRSET*, 4(1), 841-846
- [19]. Ramola, R.C., Choubey, V.M., Ganesh, P., Gusain, G.S., Tosheva, Z. and Kies, A. (2011). Radionuclide Analysis in the Soil of Kumaun Himalaya, India, Using Gamma Ray Spectrometry. *Current Science*, 100 (6): 25
- [20]. Patel, J.P. (1991). Environmental Radiation Survey of the Area of High Background Radioactivity of Mrima Hill of Kenya, *Discovery and Innovation* 3(3): 31-36.
- [21]. Achola, S.O., Patel, J.P., Mustapha, A.O. and Angeyo, H.K. (2012). Natural Radioactivity in the High Background Radiation Area of Lambwe East, Southwestern Kenya, *Radiation Protection Dosimetry*, 2, 1-6.
- [22]. Otswana, D., Patel, J.P., Bartilol, S.K. and Mustapha, A.O. (2013). Estimation of Annual Effective Dose and Radiation Hazards Due to Natural Radionuclides in Mount Homa, Southwestern Kenya, *Radiation Protection Dosimetry*, 2013: 1-8.
- [23]. Tambo, P. S. (2014). Multivariate Characterization of Natural Radioactivity Systematics in Lake Magadi Basin Geothermal System In Relation To Quality of Trona Deposits. Msc. Thesis, University of Nairobi
- [24]. ICRP, (2007). The 2007 Recommendations of the International Commission on Radiological Protection. ICRP Publication 103. *Ann. ICRP* 37: 2-4
- [25]. Nelson, D.W., and Sommers L.E. (1996). Total Carbon, Organic Carbon, and Organic Matter: *Methods of Soil Analysis*, 2nd Ed, 539-580